SME Annual Meeting
Feb. 19 - 22, 2017, Denver, CO

Preprint 17-020

CFD MODELING OF CLOUD COVER FOR POLLUTANTS DISPERSION IN DEEP OPEN-PIT MINES UNDER ARCTIC AIR INVERSION

K. V. Raj, Univ. of Alaska-Fairbanks, Fairbanks, AK
S. Bandopadhyay, Univ. of Alaska-Fairbanks Fairbanks, AK

ABSTRACT

Air inversion is a meteorological phenomenon generally occurs during winter times. Release of pollutants below the inversion height in an open-pit mine during periods of weak winds and consequently weak vertical mixing may result in very high concentrations of primary and secondary pollutants, causing serious consequences for health and safety of miners. Mine operations cease if the concentration of NO_x or CO exceeds the threshold limit value (TLV) of the pollutants. Artificial ventilation is required to dilute the pollutants to an extent that mine workers can safely resume work.

Studies of the turbulence parameters suggest that effective ventilation of the pit and removal of pollutants can be accomplished if a large enough mixing length in the open pit can be created. Turbulent mixing by eddies of different length scales under an inversion layer is product of wind shear, thermal gradient and buoyancy. The main result of turbulence is mixing of the atmospheric profile and transport of momentum. Computational fluid dynamics (CFD) Simulation results of a novel mitigation approach using cloud cover will be presented in this paper.

INTRODUCTION

In extreme climatic conditions, deep open-pit mines tend to trap pollutants at the pit bottom due to air inversions. Keeping open pits adequately ventilated is a considerable challenge for the mining community. Mine operators in cold regions are very familiar with this problem, the severity of which can be judged from Figures 1 and 2. The top portion of the figures show clear sky and snow covered benches. The brown haze, containing various contaminants accumulated over time in the pit under the air inversion, can be seen in the bottom portion of the figures. Several Arctic or subarctic mines have reported air inversions. Even Rio Tinto's Bingham Canyon pit in Utah has reported local air inversions from time to time [1].

Figure 1. Typical Air Inversion at an Open-Pit Mine, View 1.

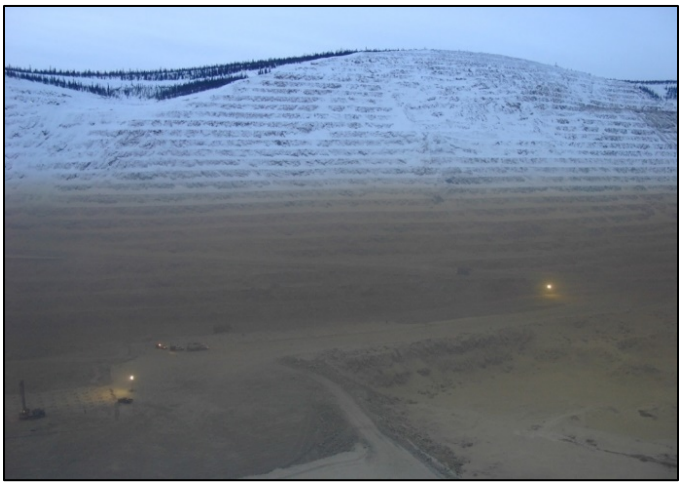

Figure 2. Typical Air Inversion at an Open-Pit Mine, View 2.

Mitigation of pollutants in deep open-pit mines in the Arctic is a challenging task. Release of pollutants below the inversion height in an open-pit mine during periods of weak winds and consequently weak vertical mixing may result in very high concentrations of primary and secondary pollutants, causing serious consequences for human health. Mine operations cease if the concentration of any one of the pollutants (NOx or CO) exceeds the TLV. Sustained cessation of a mine operation has serious economic consequences. For continued mining operation, the levels of pollutants must be below the TLVs.

If no significant synoptic meteorological situation changes during an inversion, a warm air mass sits over the cold air mass within the open pit. Artificial ventilation is required to dilute the pollutants to an extent that mine workers can safely resume work. Some of the early approaches in artificially ventilating open pits were attempted in the USSR. Most of the studies by Soviet researchers suggested the use of turbojets and turbo-propeller engines, airscrews, axial pit fans, and meteotrons [2, 3]. However, the majority of these studies were only theoretical in nature, with no evidence of an approach that really worked in practice.

Control of the atmospheric boundary layer (ABL) to ventilate open pit mines was also suggested by Belousov [4], by allowing the laminar zone to increase and reducing the recirculation zone. He proposed to install flat wings at the windward side of a pit to control the airflow entering the pit. Baklanov and Rigina [5] presented a numerical study for analyzing the effectiveness of cascade ventilation systems in open-pit mines. Another study of Belousov [6] suggested the use of breeze circulation in the pits by artificially creating a thermal gradient of 5 to 10 °C between the air mass over the pit and its surrounding areas at the same elevation. Kosarev, Timukhin [7] presented a theoretical overview of a jet-suction scheme for ventilation of stagnant zones in deep open pits. Their focus was on the lower part of the pit where air is stagnant, and where most mining activities are performed. The proposed theoretical approach, however, was neither modeled numerically, nor tested in practice.

Collingwood and others [8] provided a 2D CFD model of an actual pit geometry. The CFD modeling approach was first to model

contaminant transport under inversion, and later analyzed the effectiveness of various combinations of fans in exhaust mode to mitigate pollutants. In their model, a single pollutant source and an exhaust fan were analyzed. Their analysis suggested that the use of mechanical ventilators results in local mixing of air and dilution of pollutant concentrations. It can be seen from this brief summary of previous studies that several approaches have been suggested, but none of the approaches were field tested. Therefore, the efficacy of any of these approaches is questionable at best.

The main boundary layer forcings during inversions in an open pit are due to the pressure gradient force, the Coriolis force, cloud cover, and free flow stability. A detailed discussion on the ABL and different types of inversion layer is beyond the scope of this paper, and can be found elsewhere [9]. An increased wind speed, for example, will enhance turbulent mixing and result in reduced stratification (which can also occur due to incoming clouds). In a very stable regime, reduced stratification might result in increased surface sensible heat flux. This will alter the surface temperature and therefore the outgoing longwave radiation and stratification.

Apart from the large-scale dynamics (i.e., pressure gradient and Coriolis force), the physics that govern the structure of the wind speed and temperature profiles is complex and involves several processes with many positive and negative feedbacks. These physical processes are turbulent mixing, radiative heat transport and heat supply from underlying soil toward the surface.

Studies of the turbulence parameters (Ri, TKE, etc.) suggest that effective ventilation of the pit and removal of pollutants can be accomplished if a large enough mixing length in the open pit can be created [10]. Turbulent mixing by eddies of different scales in the SBL is produced by wind shear and dissipated by molecular viscosity and buoyancy destruction. The main result of turbulence is mixing of the atmospheric profile and transport of momentum. However, turbulent mixing in the ABL is a highly nonlinear process. The TI is influenced by wind shear and stratification.

Several approaches can be examined that may create a large mixing length. One of the approaches could be to create local dilution within a working area of the pit, such that the pollutant concentrations are well below the TLV, while other areas in the pit could be above the TLV. The second approach is to clear the entire pit of any pollutant that is above the TLV. This can be achieved by creating cloud cover over the pit which results in radiation balance to be positive and thermal forcing strong enough to break the inversion. This paper presents the CFD modeling of the cloud cover over an open pit.

DISPERSION OF POLLUTANTS USING CLOUD COVER

Before presenting the details of CFD modeling and results, it is important to understand the mechanism by which cloud cover assists in breakage of inversion layer and how the authors came to the conclusion that cloud cover could lift the inversion layer in an open pit mine.

It has been observed that, during snowfall in the open pit, the inversion lifts and the pit is cleared of all pollutants. Thus, it is initially hypothesized that heat released from the snowflakes lifts the inversion. A critical examination of the weather and radiation data suggest that breakup of the inversion layers can happen with or without snowfall.

On further investigation it was found that it is not the snowfall, but the presence of low-level cloud cover that lifts the inversion. The presence of low-level clouds results in snowfall or rain. These low-level cloud covers are sensitive to infrared radiation. Since all objects (including the earth's surfaces and cloud covers) emit radiation, properties such as emissivity and reflectivity play a significant role in changing the thermal regime of air between the ground surface and the clouds. Since clouds are infrared sensitive they reflect most of the infrared radiation emitted from the ground. Similarly, the snow-covered ground reflects most of the radiation back to the cloud cover (Liou 2002). Clouds, when present, are the major contributors to incoming longwave radiation to the ground surface. They radiate like blackbodies (low-level clouds are regarded as a blackbody, $\varepsilon \approx 1$) at their respective cloud base temperatures. However, some of the radiation is absorbed by water vapor, CO_2, and other greenhouse gases before reaching the earth's surface [11]. The temperature and emissivity differences between the air layers, as well as the difference in the emitted and absorbed longwave radiation between the layers, results in a net radiative flux.

In the stable boundary layer (SBL), the temperature gradient near the ground surface can be extremely large. Radiative heat transport is a complex process of absorption and emission of thermal radiation (by absorbers) in the atmospheric layers relative to each other, and to and from the ground surface. The net effect of radiation emission and reflection results in a state of equilibrium of temperature in the cloud cover, as well as at the ground surface. This state of equilibrium leads to the change in vertical temperature profile of the air. The state of temperature equilibrium under cloud cover is validated by data collected by infrared sensors at the selected mine. The collected incoming and outgoing infrared radiation data are presented in Figure 3 and Figure 4. It can be seen from Figure 3 that the incoming and outgoing infrared radiation at the pit bottom tend to overlap each other at around 6:00 AM (October 29, 2013), whereas at the pit rim (Figure 4), the incoming and outgoing radiation values do not overlap, although they are very close. The magnitude of the incoming and outgoing radiation are near zero (W/m^2). This is a clear indication that a cloud is passing over the sensors.

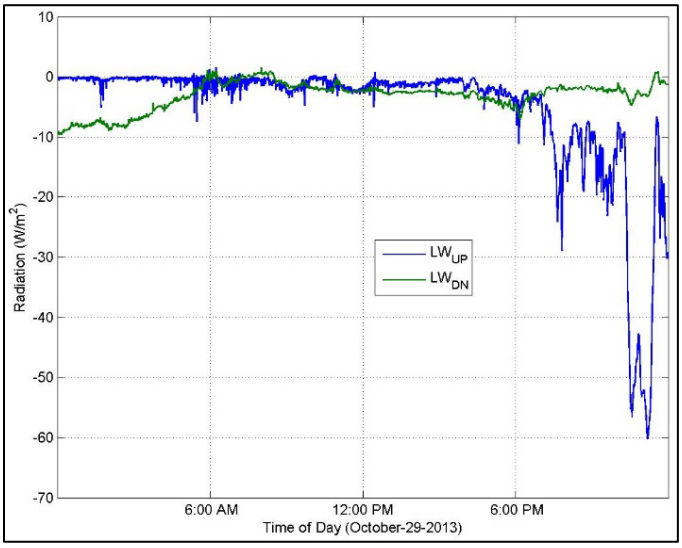

Figure 3. Infrared Radiation Measurements at Pit Bottom during Cloud Cover (October 29, 2013).

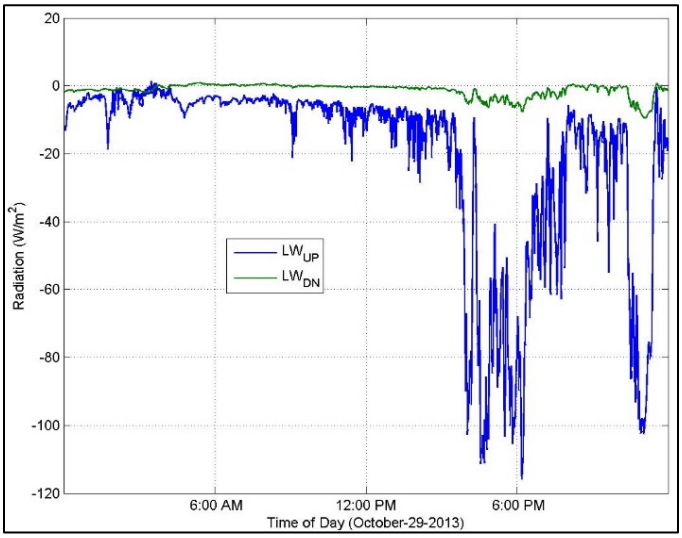

Figure 4. Infrared Radiation Measurements at Pit Rim during Cloud Cover (October 29, 2013).

Other clear evidence of cloud cover over the selected open pit is presented in Figure 5, in the form of base reflectivity RADAR data from the same date. Weather RADARs are the most commonly used instrument for detecting water content in the atmosphere. The area enclosed in the rectangle (Figure 5) is the selected mine, and the green shading over it indicates the presence of cloud cover.

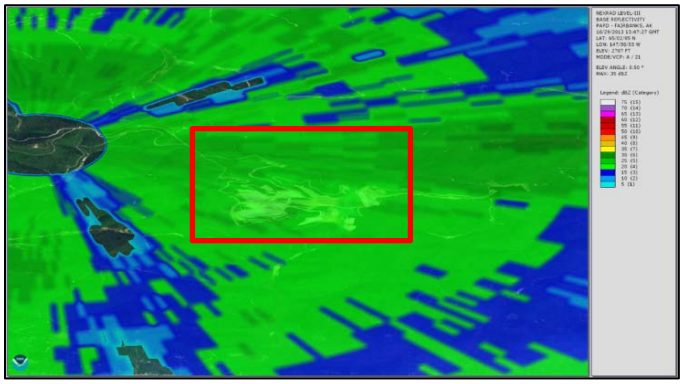

Figure 5. RADAR Base Reflectivity Data on October 29, 2013 (http://www.ncdc.noaa.gov/nexradinv/).

Formation of cloud/fog is related to air and dew point temperatures. The dew point temperature is the temperature at which the vapor pressure becomes saturated via the isobaric (constant pressure) cooling process [12]. Once the air temperature drops to the dew point temperature, the vapor becomes saturated and the excess water vapor starts to condense. It can therefore be stated that when there is convergence of air temperature with dew point temperature, cloud/fog formation occurs.

Additional evidence of cloud cover in the surrounding area of the selected open pit are presented in Table 1 and Table 2. Air and dew point temperatures and relative humidity data are provided in Table 1 and Table 2 for two weather stations located near the selected open pit. The weather stations are identified as Weather Station 1 (WS 1) and Weather Station 2 (WS 2). WS 1 has a similar elevation (2267 ft/691 m) as that of the west rim of the selected open pit and WS 2 is at a similar elevation (2099 ft/ 640 m) as the east side of the pit rim. It can be observed from the WS 1 data in Table 8.1 that the water vapor in the atmosphere has reached saturation (the daily average temperature and the dew point temperature are the same and relative humidity is 100%). At WS 2, the daily average temperature and the dew point temperature are very close (difference of 0.55°C), with a relative humidity of 96%.

Table 1. Weather Station 1 Data on October 29, 2013 (http://www.wunderground.com/).

	High	Low	Average
Temperature (°C)	1.67	-1.67	-0.67
Dew Point (°C)	1.67	-1.67	0.67
Relative Humidity (%)	100	100	100

Table 2. Weather Station 2 Data on October 29, 2013 (http://www.wunderground.com/).

	High	Low	Average
Temperature (°C)	1.11	-2.78	-1.06
Dew Point (°C)	0.56	-3.33	-1.61
Relative Humidity (%)	96	95	96

Additional data from various dates were selected to provide support for the discussions presented above (Figure 6 through Figure 11 and Table 3 through Table 6). Analysis of the data indicates that there is a change in the infrared radiation during cloud cover. The presence of cloud cover results in convergence of the incoming and the outgoing longwave radiation values to zero, thus providing a basis for modeling the presence of cloud cover over an open pit. It must be noted that, in practice, longwave radiation values cannot be exactly zero. The values presented in Figure 3 and Figure 4 are the longwave radiation values minus the longwave radiation emitted from the sensor.

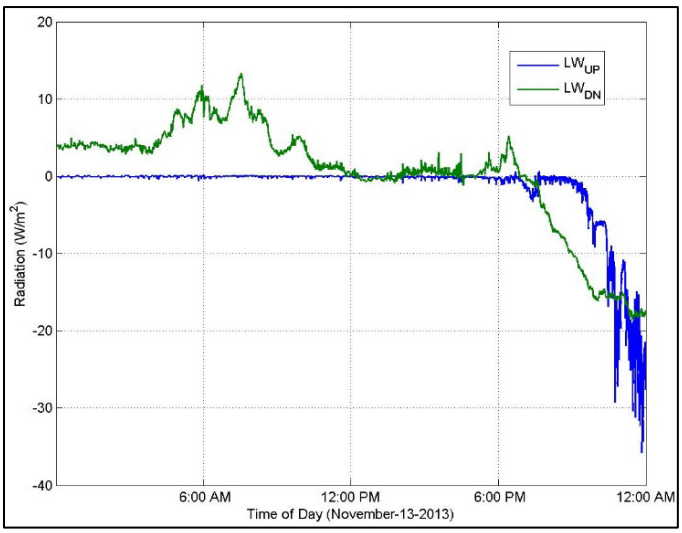

Figure 6. Infrared Radiation Measurements at Pit Bottom during Cloud Cover (November 13, 2013).

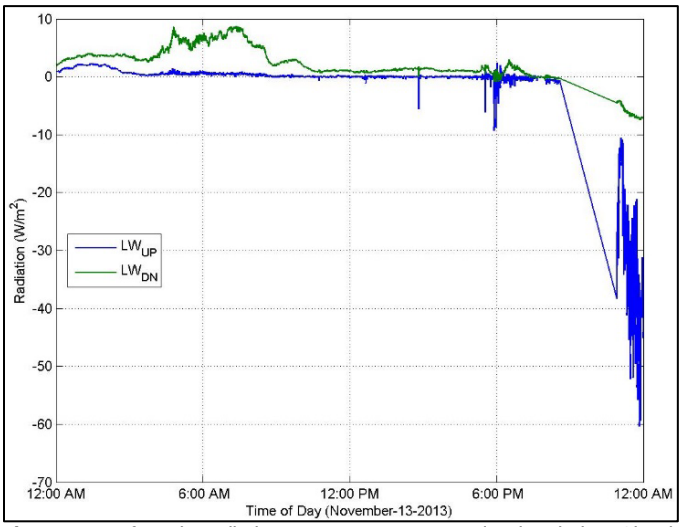

Figure 7. Infrared Radiation Measurements at Pit Rim during Cloud Cover (November 13, 2013).

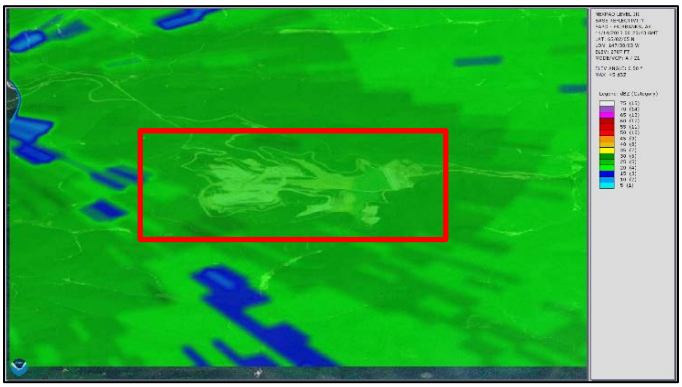

Figure 8. RADAR Base Reflectivity Data on November 13, 2013 (http://www.ncdc.noaa.gov/nexradinv/).

Contrary to the data presented above, another set of data (November 20, 2013) is presented below for when there is an absence of cloud cover. The relevant data (temperature, radiation, etc.) are different in the absence of cloud cover. Figure 12 shows infrared radiation data for the pit bottom and pit rim infrared radiation data are presented in Figure 13. It can be seen from these data that the incoming and

outgoing infrared radiation are apart from each other. The difference between the incoming and outgoing radiation, therefore, is nonzero. The absence of cloud over the sensors during that time can be verified from the satellite (Figure 14) of the selected open-pit mine on November 20, 2013, which clearly indicates a cloud-free day.

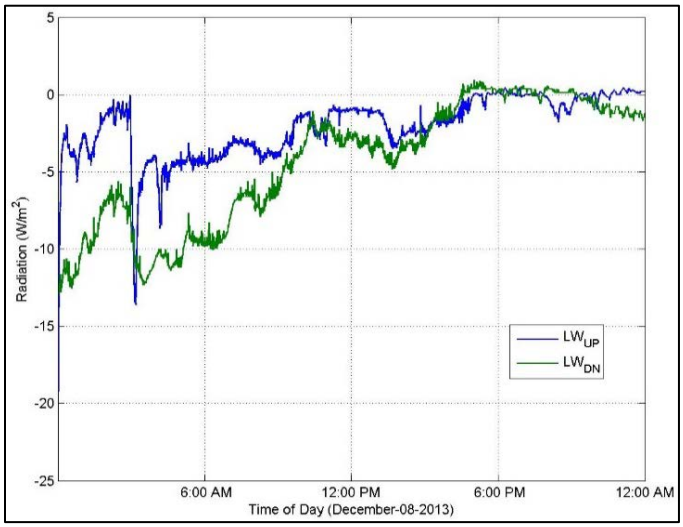

Figure 9. Infrared Radiation Measurements at Pit Bottom during Cloud Cover (December 8, 2013).

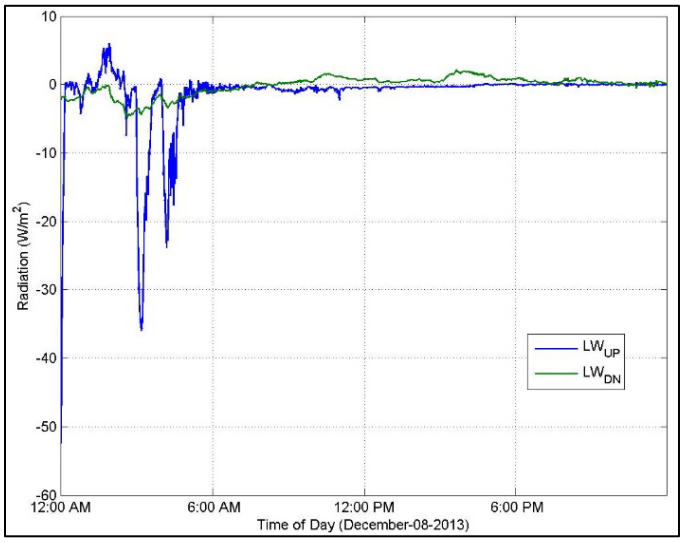

Figure 10. Infrared Radiation Measurements at Pit Rim during Cloud Cover (December 8, 2013).

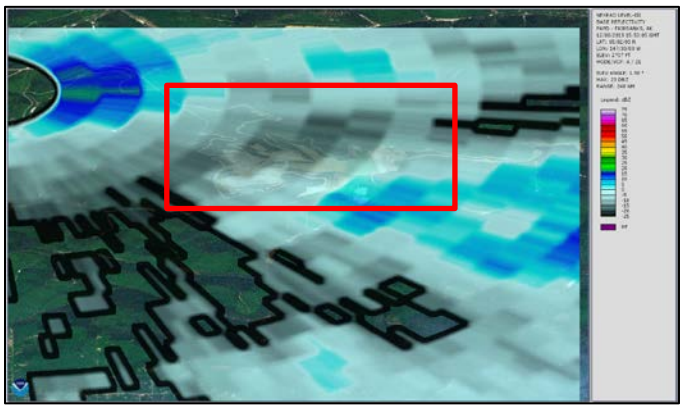

Figure 11. RADAR Base Reflectivity Data on December 8, 2013 (http://www.ncdc.noaa.gov/nexradinv/).

Table 3. Weather Station 1 Data on November 13, 2013 (http://www.wunderground.com/).

	High	Low	Average
Temperature (°C)	0.0	-13.89	-9.17
Dew Point (°C)	0.0	-15.56	-10.5
Relative Humidity (%)	100	86	90

Table 1: Weather Station 2 Data on November 13, 2013 (http://www.wunderground.com/).

	High	Low	Average
Temperature (°C)	1.67	-13.38	-8.67
Dew Point (°C)	1.67	-14.44	-8.83
Relative Humidity (%)	100	92	99

Table 5. Weather Station 1 Data on December 8, 2013 (http://www.wunderground.com/).

	High	Low	Average
Temperature (°C)	0.56	-1.67	-1.00
Dew Point (°C)	-0.56	-2.78	-1.72
Relative Humidity (%)	96	92	95

Table 6. Weather Station 2 Data on December 8, 2013 (http://www.wunderground.com/).

	High	Low	Average
Temperature (°C)	0.0	-1.67	-0.89
Dew Point (°C)	0.0	-1.67	-0.89
Relative Humidity (%)	100	100	100

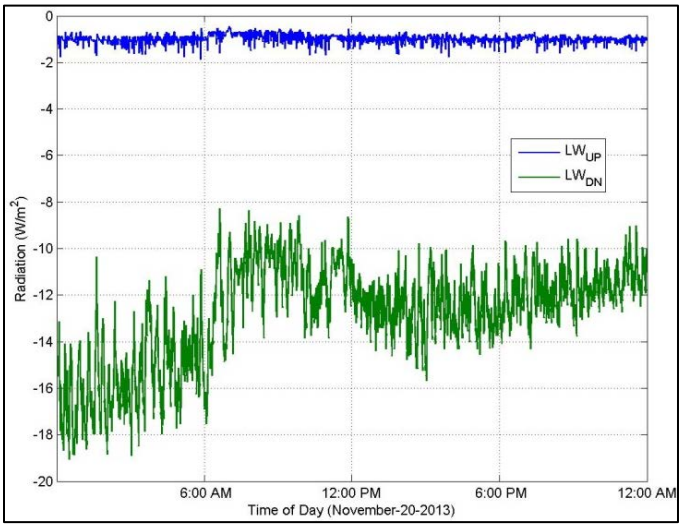

Figure 12. Infrared Radiation Measurements at Pit Bottom with No Cloud Cover (November 20, 2013).

Data from WS 1 and WS 2 on the same date also indicate the absence of cloud cover in the surrounding area of the open-pit mine. The data from WS 1 and WS 2 are presented in Table 7 and Table 8. It is evident from both tables that the air and dew point temperatures are different, thus, indicating the absence of cloud cover near the sensors.

From the data above, a conclusion can be made that during an atmospheric inversion, advancing clouds or formation of clouds play an important role in changing vertical temperature profiles. It is hypothesized that introduction of cloud cover over the open-pit mine could lift the inversion. The presence of cloud cover was therefore simulated for mitigation of contaminants under inversion.

CFD MODEL SETUP AND INTRODUCTION OF CLOUD COVER IN THE MODEL DOMAIN

A detailed description of the CFD models, meshing and mesh optimization, and validation of the models are not included here, it can however, be found elsewhere [13, 14]. In order to examine the effects of cloud cover, the 2013 pit geometry was selected for the mitigation simulation model. The results after 13 hr of simulation with the realizable

κ-ε turbulence model was used as the initial condition. Details of the realizable κ-ε turbulence model for 2013 pit geometry can be found elsewhere [14].

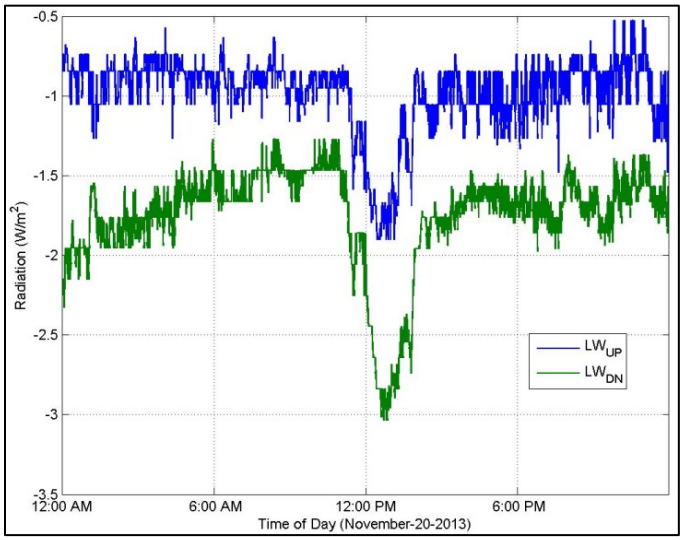

Figure 13. Infrared Radiation Measurements at Pit Rim with No Cloud Cover (November 20, 2013).

Figure 14. Satellite Image on November 20, 2013 (http://www.ncdc.noaa.gov/nexradinv/).

Table 7. Weather Station 1 Data on November 20, 2013 (http://www.wunderground.com/).

	High	Low	Average
Temperature (°C)	-20.00	-25.56	-22.94
Dew Point (°C)	-22.78	-27.78	-25.50
Relative Humidity (%)	80	75	79

Table 8. Weather Station 2 Data on November 20, 2013 (http://www.wunderground.com/).

	High	Low	Average
Temperature (°C)	-20.00	-23.89	-22.22
Dew Point (°C)	-20.56	-25.00	-22.83
Relative Humidity (%)	96	92	94

The data collected from the pit bottom radiation sensor (December 7, 2013) were used in the simulation. The cloud cover was introduced in the model once the inversion set in.

From the infrared radiation data presented in Figure 3, Figure 4, Figure 6, Figure 7, Figure 9 and Figure 10, it is clear that under cloud cover the incoming and the outgoing infrared radiation values tend to coincide near zero (W/m^2).

The SBL in an open-pit mine is sensitive to the radiation balance [9]. This boundary layer cools at the surface due to the net negative radiation balance. In the absence of cloud cover, the clear sky gives rise to strong radiative cooling. When a cloud arrives, the surface temperature and the relative humidity increase. The outgoing longwave radiation follows these temperature oscillations.

The introduction of cloud cover was reflected by setting the heat fluxes in the model domain top wall boundary (the top of the temperature inversion), FA, and the bottom wall boundary, PIT, to zero (W/m^2) [15]. The incoming and outgoing solar (shortwave) radiation were assumed to be low and were neglected. In the absence of solar radiation, the heat fluxes are only due to the infrared radiation. The sensors at the selected mine collect data every ten seconds. For the stability of the model, the data were averaged over a 4-hr time period and used in the model to replicate the changing weather conditions. All other model parameters were kept unchanged. Input of varying temperature, velocity, and radiation/heat flux data every 4 hr changes the boundary conditions in the model. Figure 15 through Figure 20 show the development of the inversion in the open-pit mine over a 6-hr time period. The resulting NO_2 concentration during this 6-hr period envelope the entire open pit. The velocity vector of the initial state (t≈13.69 hr) shows that the flow from east to west in the pit is streamlined. However, development of the inversion during this time period results in low air velocity in the high contaminant zones.

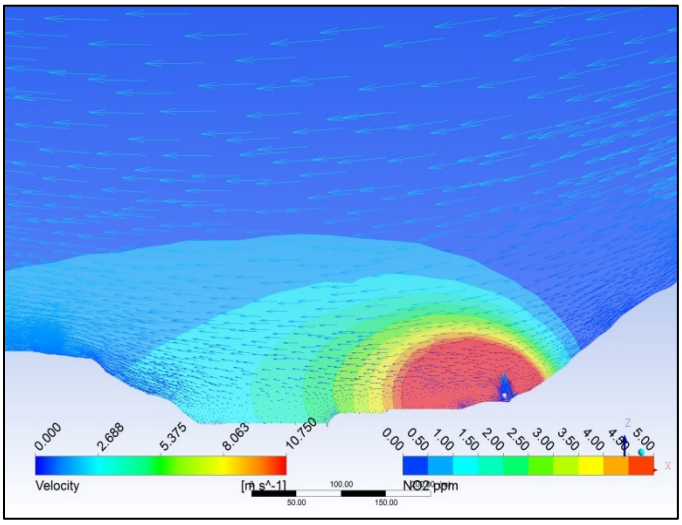

Figure 15. Contours of NO_2 Concentrations (ppm) and Velocity Vectors in Vertical Plane along East-West Direction (t ≈ 13.69 hr).

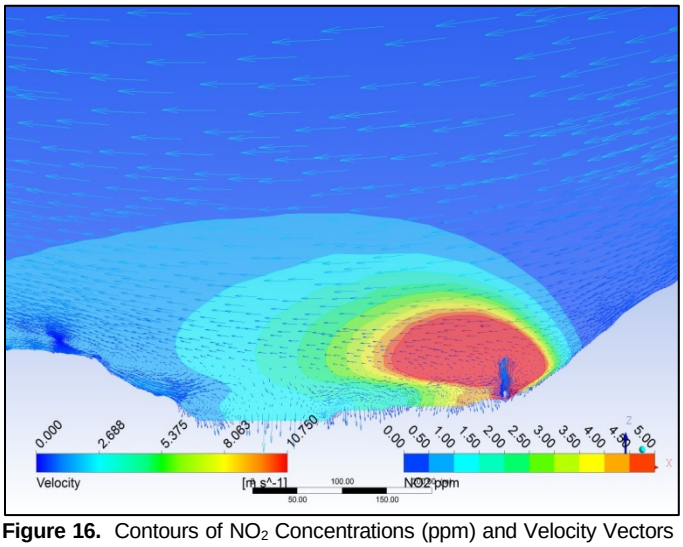

Figure 16. Contours of NO_2 Concentrations (ppm) and Velocity Vectors in Vertical Plane along East-West Direction (t ≈ 14.69 hr).

Figure 20 shows that the open pit is under strong inversion and there is a high level of NO_2 (above 5 ppm) in the entire pit. This pit, with high levels of NO_2 and an initially stratified boundary layer, was selected for mitigation modeling using cloud cover.

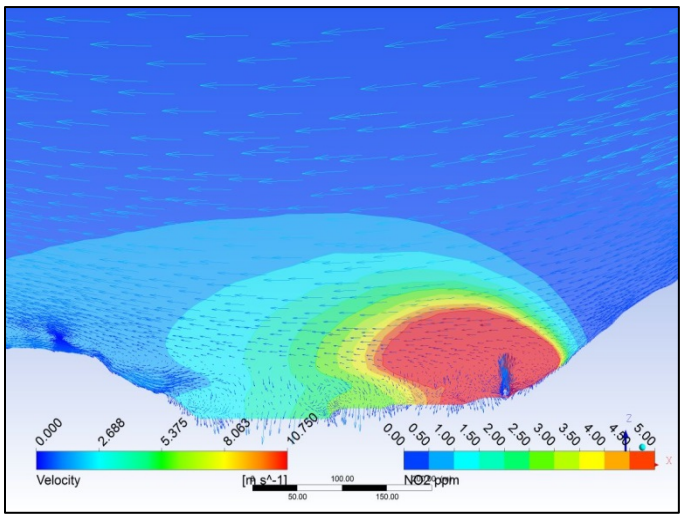

Figure 17. Contours of NO_2 Concentrations (ppm) and Velocity Vectors in Vertical Plane along East-West Direction (t ≈ 15.69 hr).

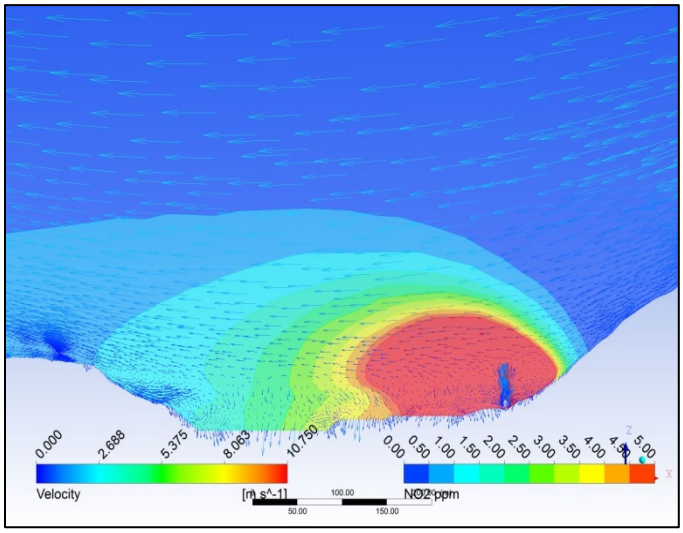

Figure 18. Contours of NO_2 Concentrations (ppm) and Velocity Vectors in Vertical Plane along East-West Direction (t ≈ 16.69 hr).

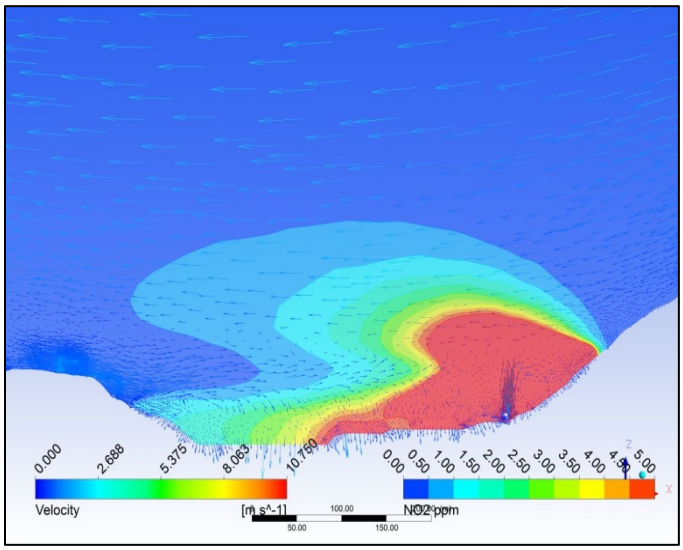

Figure 19. Contours of NO_2 Concentrations (ppm) and Velocity Vectors in Vertical Plane along East-West Direction (t ≈ 17.65 hr).

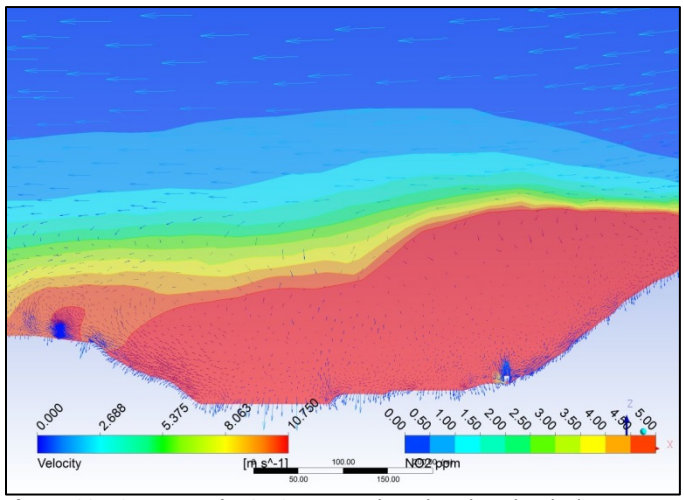

Figure 20. Contours of NO_2 Concentrations (ppm) and Velocity Vectors in Vertical Plane along East-West Direction (t ≈ 18.65 hr).

Cloud cover was introduced in the model domain by changing the heat fluxes at the top and the bottom walls to zero (W/m^2). Figure 21 and Figure 22 show the changing level of NO_2 concentration after the introduction of cloud cover in the model domain. It can be seen that within 2 hr, the concentration of NO_2 is 3 ppm or less, which is well below the TLV.

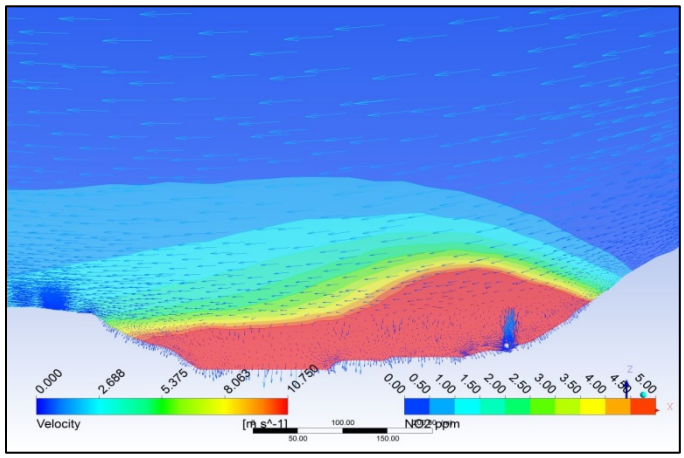

Figure 21. NO_2 Concentrations (ppm) and Velocity Vectors in Vertical Plane along East-West Direction (t ≈ 19.65hr).

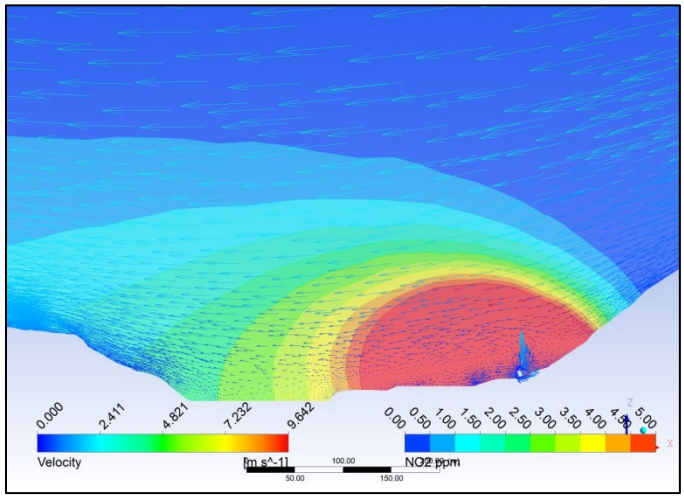

Figure 22. NO_2 Concentrations (ppm) and Velocity Vectors in Vertical Plane along East-West Direction (t ≈ 20.31hr).

Figure 23 and Figure 24 show temperature and NO_2 concentration, respectively, as a function of time. Changes in the temperature profile are clearly visible from Figure 24; following the introduction of cloud cover, the vertical temperature gradient changes from a positive value to a negative value, indicating breakup of the inversion. From Figure 24 it can be seen that the NO_2 concentration increase from 2 ppm (t ≈ 16.69 hr) to 9 ppm (t ≈ 18.65 hr). With the introduction of cloud cover, however, it decreases to around 3 ppm (t ≈ 20.31 hr). Thus, it can be stated that introduction of cloud cover over the open pit changes the vertical temperature profile, resulting in the breakup of the SBL and dilution of pollutants to concentrations below the TLV.

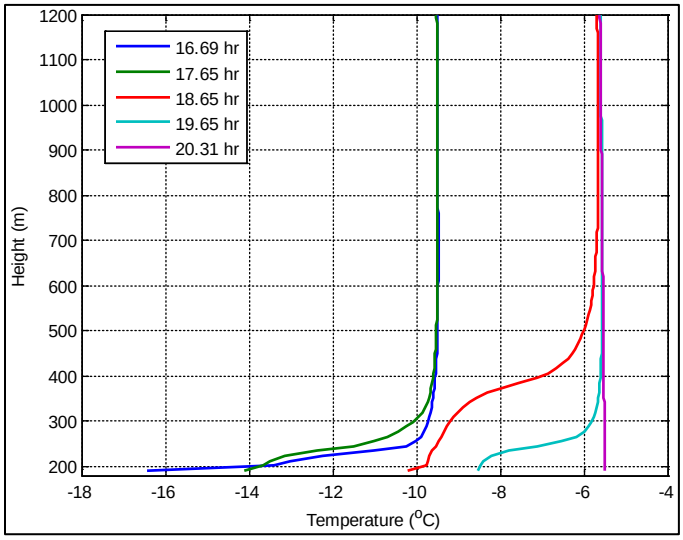

Figure 23. Temperature Profiles along the Vertical Line.

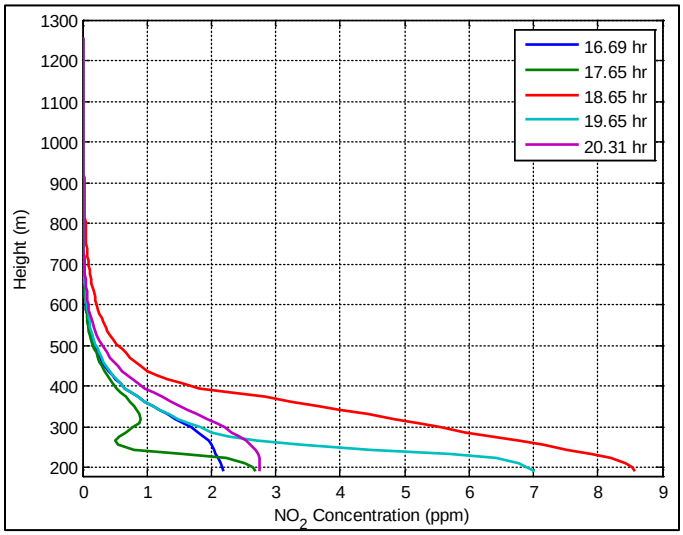

Figure 24. NO_2 Concentrations (ppm) along the Vertical Line.

The simulated model results show that cloud cover over the open-pit mine changes the vertical temperature profiles. The results presented above show that within a couple of hours the pit is cleared of high NO_2 concentrations. Other factors, however, such as elevation, extent of cloud cover over the area, and thickness of cloud cover over the pit, may influence the amount of time needed for breakup of the inversion and removal of pollutants from the pit.

CONCLUSIONS

Mitigation of pollutants in deep open-pit mines under air inversion in the Arctic is a challenging task. Release of pollutants below the inversion height in an open-pit mine during periods of weak winds and consequently weak vertical mixing may result in very high concentrations of primary and secondary pollutants, causing serious consequences for miners' health. Any solution to reduce the pollutant concentrations requires to create mixing length large enough to disperse the pollutants to the length of inversion layer and beyond.

A novel approach using cloud cover to disrupt the inversion was modeled which creates thermal forcing large enough to dilute the pollutant concentrations to values lower than the TLVs. This approach is based on infrared data collected at the selected open -pit mine. Introduction of cloud cover led to lifting or disruption of the inversion, and consequently the removal of pollutants from the pit. The 2013 pit configuration results indicated that the pit would be cleared of all pollutants in approximately 2 hr.

ACKNOWLEDGEMENTS

The authors would like to acknowledge the National Institute for Occupational Safety and Health (NIOSH) for the financial support from a NIOSH Research Contract # 200-2009-31968. The authors would also like to acknowledge Mr. Chris Pritchard of NIOSH for his valuable suggestions and feedback on the research. Assistance provided by the ANSYS technical support staff and mining engineers at the selected open pit mine is also gratefully acknowledged.

REFERENCES

1. Whiteman, C.D. and S.W. Hoch, *Bingham Mine Cold-Air Pool Structure and Evolution*. 2014, Department of Atmospheric Sciences, University of Utah: Salt Lake City, Utah.
2. Vershinin, A.A., *Comparative assessment of schemes for artificial ventilation of quarries.* Soviet Mining, 1976. 12(6): p. 627-630.
3. Parakhonskii, É.V. and L.P. Severin, *High-efficiency ventilator plants for artificial ventilation of deep open-cut mines.* Soviet Mining, 1976. 12(6): p. 665-670.
4. Belousov, V.I., *Ventilation of Open-Pit Mines by Controlling the Boundary Layer of the Wind Stream.* Soviet Mining, 1989. 25(3): p. 267-270.
5. Baklanov, A.A. and O.Y. Rigina, *Effectiveness of Cascade Ventilation Systems for Open-Pit Mines.* Journal of Mining Science, 1993. 29(2): p. 152-157.
6. Belousov, V.I., *Breeze Circulation in Open-Pit Mines.* Journal of Mining Science, 1995. 31(3): p. 216-220.
7. Kosarev, N.P., et al., *Aerodynimcs of Jet-Suction Scheme for Ventilation of Deep Open-Pit Stagnant Zones.* Izvestiya Vysshikh Uchebnykh Zavedenii, Gornyi Zhurnal [in Russian], 2005(6): p. 16-19.
8. Collingwood, W., K.V. Raj, and S. Bandopadhyay. *CFD Modeling of Pollution Transport in Open Pit Mines under Arctic Air Inversion*. in *Proceedings of the 14th U. S. /North American Mine Ventilation Symposium*. 2012. Salt Lake City, Utah: University of Utah,
9. Raj, K.V., G.J. Fochesatto, and S. Bandopadhyay. *Air Temperature Inversions and its Impact on Natural Ventilation in Open pit Mines*. in *Proceedings of the 15th North American Mine Ventilation Symposium*. 2015. Blacksburg, VA: Department of Mining and Minerals Engineering,
10. Bandopadhyay, S., K.V. Raj, and R.V. Ramani. *A Three-Dimensional CFD Model of Pollutant Transport in a Deep Open-Pit Mine under Arctic Air Inversion*. in *Proceedings of the Tenth International Mine Ventilation Congress*. 2014. Sun City, South Africa: The Mine Ventilation Society of South Africa.
11. Arya, P.S., *Introduction to Micrometeorology*. Vol. 79. 2001: Academic press.
12. Wang, P.K., *Physics and dynamics of clouds and precipitation*. 2013: Cambridge University Press.
13. Raj, K.V., W. Collingwood, and S. Bandopadhyay, *Challenges in CFD Modeling of Air Flow in Open-Pit Mines.* Transactions of the

Society for Mining, Metallurgy, and Exploration, 2013. 334: p. 449-456.

14. Raj, K.V. and S. Bandopadhyay. *CFD Model Validation of Pollutant Transport in Open Pit Mine under Air Inversion*. in *SME Annual Meeting*. 2016. Phenix, AZ: SME, Preprint No. TP-16-067.
15. Raj, K.V., S. Bandopadhyay, and R.V. Ramani, *Turbulent Models for Pollutant Transport in Open Pit Mines under Stable Boundary Layer.* Transactions of the Society for Mining, Metallurgy, and Exploration, 2015. 338: p. 96-106.